

Piezoresistive Microcantilever Optimization for Uncooled Infrared Detection Technology

S. Rajic[†], B.M. Evans III[†], P.G. Datskos^{*,#}, P.I. Oden^{*,#}, T. Thundat[†], and C.M. Egert[†]

[†]*Oak Ridge National Laboratory, Oak Ridge, Tennessee, 37831*
and

[#]*University of Tennessee, Department of Physics, Knoxville, TN 37996-1200,*

ABSTRACT

Uncooled infrared sensors are significant in a number of scientific and technological applications. A new approach to uncooled infrared detectors has been developed using piezoresistive microcantilevers coated with thermal energy absorbing material(s). Infrared radiation absorbed by the microcantilever detector can be sensitively detected as changes in the electrical resistance as a function of microcantilever bending. These devices have demonstrated sensitivities comparable to existing uncooled thermal detector technologies. The dynamic range of these devices is extremely large due to measurable resistance change obtained with only nanometer level cantilever displacement. Optimization of geometrical properties for selected commercially available cantilevers is presented. Additionally, we present results obtained from a modeling analysis of the thermal properties of several different microcantilever detector architectures.

Keywords: infrared, detector, uncooled, microcantilever, piezoresistive

1. INTRODUCTION

Infrared (IR) radiation is the second most intense radiation band in our environment and its detection and imaging has extensive military, industrial, and commercial applications, such as remote monitoring of facilities and equipment, process control, surveillance, night-vision, collision avoidance, and medical imaging. Presently, there is a number of families of commercially available IR detectors, including thermopiles, pyroelectrics, bolometers, and various solid state detectors¹⁻⁶. Thermopile detectors typically have a large thermal mass and long response times (> 10 ms). Bolometers using micromachined, suspended foils have much better rise times due to their reduced mass and thermal conductivity. Pyroelectrics and bolometers offer broad spectral response when coated with suitable IR absorbing materials. Solid state detectors for the IR region, such as quantum well devices, must generally be operated at reduced temperatures due to inherently high thermal noise. Additionally, the spectral response of these semiconductor devices is limited by the intrinsic properties of the composing materials. These infrared detectors can be classified either as quantum detectors - such as the photoconductors; or thermal detectors - such as bolometers and pyroelectrics. For the former type, incident infrared radiation is converted into an electronic response while with thermal detectors, IR radiation is converted into heat which is subsequently detected through temperature changes. Depending on the operational demands, one type of detection device may be favored over another; as a general rule, when the photon energy of the infrared radiation $h\nu > k_B T$, photon detectors offer better performance and when $h\nu < k_B T$, thermal detectors are generally favored.

A new approach for producing compact, light-weight, highly-sensitive micromechanical IR detectors is provided by microcantilever technology which is based on the bending of a microcantilever as a result of absorption of IR energy⁷. When a microcantilever is exposed to infrared radiation, the temperature of the microcantilever rises due to absorption of this energy. If bimaterial microcantilevers are constructed from materials exhibiting dissimilar thermal expansion properties (such as silicon nitride coated with a thin gold film), the bimaterial effect will cause the microcantilever to bend in response to this temperature variation. The extent of bending is directly proportional, in first order, to the

rate of energy absorption, which, in turn, is proportional to the radiation intensity. Previous work has shown that microcantilever bending can be detected with extremely high sensitivity⁸⁻¹⁰. For example, metal-coated microcantilevers that are commonly employed in atomic force microscopy (AFM) allow sub-Angstrom ($< 10^{-10}$ m) sensitivity to be routinely obtained. Recent studies have reported¹¹⁻¹⁴ the use of microcantilever bending for calorimetric detection of chemical reactions with energies as low as a few pJ. It was demonstrated¹⁴ that a similar detector had an observed sensitivity of 100 pW corresponding to an energy of 150 fJ and use of the sensor as a femtojoule calorimeter was proposed. An estimate of the minimum detectable power level was on the order of 10 pW, corresponding to a detectable energy of 10 fJ and a temperature sensitivity 10^{-5} K. However, using an optimally designed microcantilever, the sensitivity may be improved even further. Hence, for applications in optical radiation detection,

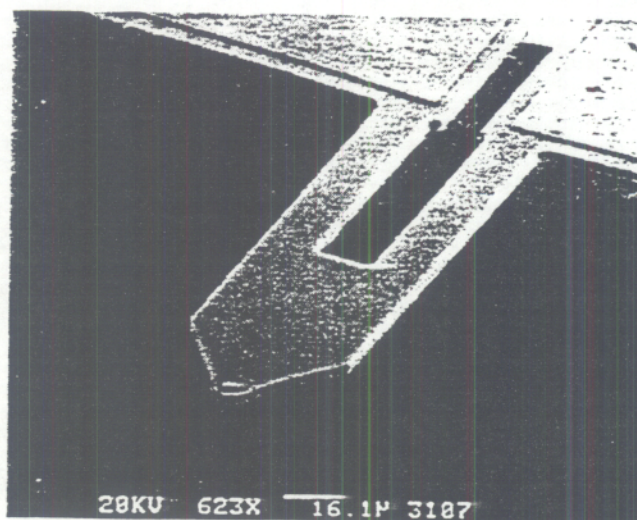


Figure 1. Electron scanning micrograph of a piezoresistive microcantilever used in the present studies.

microcantilevers can be coated with appropriate absorptive materials such that they undergo bending upon exposure to radiation (such as infrared or near infrared radiation). IR sensing microcantilevers can be 50 - 400 μm long, 0.3 - 4 μm thick and 10 - 50 μm wide, and made out of materials such as silicon nitride, silicon or other types of semiconducting materials (see Fig. 1). Due to the monolithic nature of these devices, they can easily be produced in one- and two-dimensional arrays with hundreds of cantilevers on a single wafer. This type of fabrication scheme possesses obvious advantages when considering the production of infrared imaging systems with these microcantilever devices.

When considering the bending of the microcantilever, a relationship between bending and the absorbed energy by the microcantilever is obtained by assuming a spatially uniform incident power, dQ/dT , onto a bimetallic microcantilever. The maximum deflection, z_{max} , due to differential stress is given by^{14,15}:

$$z_{\text{max}} = \frac{5}{4} \frac{(t_1 + t_2)l^3}{(\lambda_1 t_1 + \lambda_2 t_2)w t_2^2} \frac{(\alpha_1 - \alpha_2)}{4 + 6 \frac{t_1}{t_2} + 4 \frac{t_1^2}{t_2^2} + \frac{E_1 t_1^3}{E_2 t_2^3} + \frac{E_2 t_2}{E_1 t_1}} \eta \left(\frac{dQ}{dt} \right) \quad (1)$$

where l and w are, the length and width of the microcantilever, respectively, t_1 and t_2 are the thicknesses of the two layers, λ_1 , λ_2 ; α_1 , α_2 ; E_1 , E_2 are the thermal conductivities; thermal expansion coefficients and Young's moduli of elasticity of the two layers; $\eta dQ/dT$ is the fraction of the radiation power absorbed. In order to increase the IR detection sensitivity of a microcantilever the maximum deflection should be maximized which is strongly dependent on the geometry and thermal properties of the two layers. In the present work we investigated the role of thickness of the microcantilever on the overall response to IR radiation.

2. MODELING

The finite element method was used to simulate energy transfer to the microcantilever and its corresponding deflection. The model consisted of 753 solid elements and 99 shell elements. Due to symmetry of the part and the

high aspect ratio of the individual layers, only half of the microcantilever was modeled. Brick elements were used to model the silicon microcantilever, the $1\mu\text{m}$ thick aluminum layer on the heat sink, and the silicon heat sink. Shell elements were used to represent the 50nm layer of gold on the microcantilever. Restraints were added to the model to enforce the symmetrical loading condition. Fig. 2 illustrates the finite element model of the microcantilever with the elements shrunken by 20% to increase the spacing between elements for clarity.

The software packages Pro/Engineer and Mechanical were used to model and solve the geometry. A thermal heat load was applied to the top surface of the microcantilever. The heat loads were used to solve for the temperature profile, and then a mechanical analysis using the resulting temperature profile was performed to obtain the mechanical response of the cantilever. Finite element analysis was also used to determine the natural frequency of the structure. A convergence of 10% was required to ensure accuracy of results.

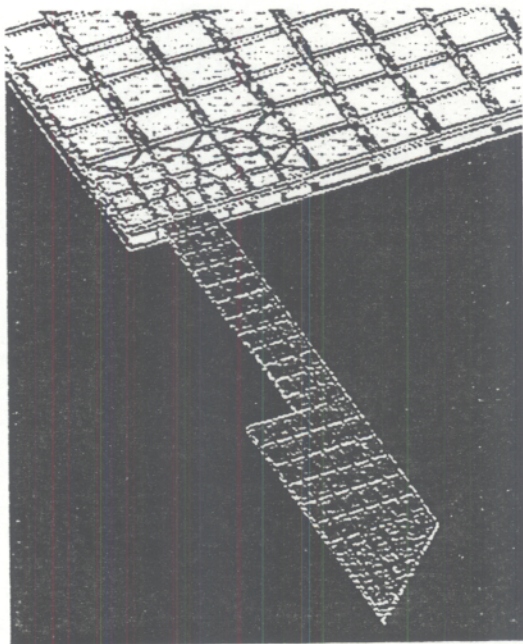


Figure 2. Finite element model of microcantilever and heat sink with increased density of elements near critical areas.

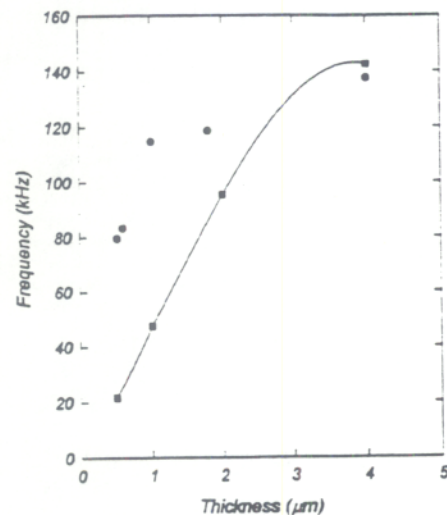


Figure 3. Resonance frequency as a function of thickness, t , of the microcantilever. The square points were obtained from finite element modeling analysis. The circles are experimentally measured values.

As can be seen from Fig. 3, the resonance frequency exhibits almost a linear dependence on the thickness of the microcantilever (with the exception of the $4\mu\text{m}$ case); actually a $t^{3/2}$ is expected⁸. The resonance frequency of the $4\mu\text{m}$ microcantilever does not follow that of the others because it has the same thickness as the heat sink and the heat sink responds with the microcantilever. In the analysis of the thinner microcantilevers, vibrational interaction with the heat sink was minimal.

Four different heat loads were applied to four different variations of the microcantilever geometry. The thickness of the cantilever was varied from $4\mu\text{m}$ to $2, 1$, and $0.5\mu\text{m}$. Heat loads of 1mW , $100\mu\text{W}$, $10\mu\text{W}$, and $1\mu\text{W}$ were applied to the microcantilever and heat sink surface of each of the geometries. Figs 4 and 5 display the thermal profile of the $1\mu\text{m}$ thick model with $100\mu\text{W}$ of applied energy and a plot of temperature versus distance along the microcantilever for all thicknesses, respectively. The cantilever surface represents 7% of the area of the entire object to which heat was applied.

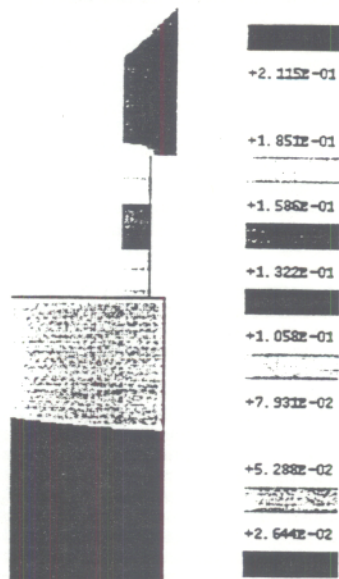


Figure 4. Temperature change for $1\mu\text{m}$ thick cantilever due to $100\mu\text{W}$ heat load over entire surface. (units degrees celsius)

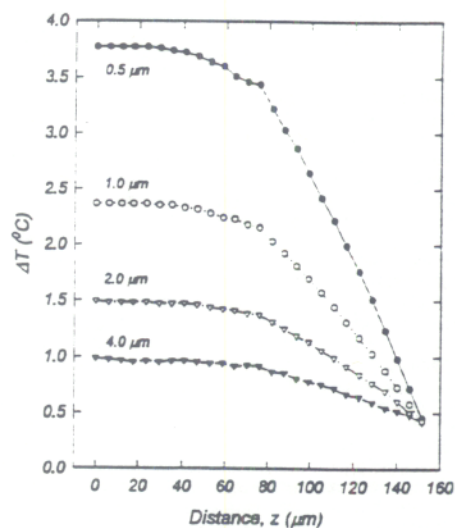


Figure 5. Temperature increase of the microcantilever as a function of distance from the base for a number of thicknesses.

Fig. 6 illustrates the deflection due to thermal distortion of the $1\mu\text{m}$ thick microcantilever for a $100\mu\text{W}$ applied heat load with the axis perpendicular to the microcantilever absorbing surface exaggerated. Thermal distortion was determined to be a function of preferential heating of the microcantilever on the surface exposed to the source. Fig. 7 plots the variation in thermal distortion to microcantilever thickness for a given intensity of $10\mu\text{W}$. The larger distortion of the $0.5\mu\text{m}$ microcantilever is mostly a function of the increase in thermal resistance and the increase in temperature change resulting from the smaller microcantilever mass.

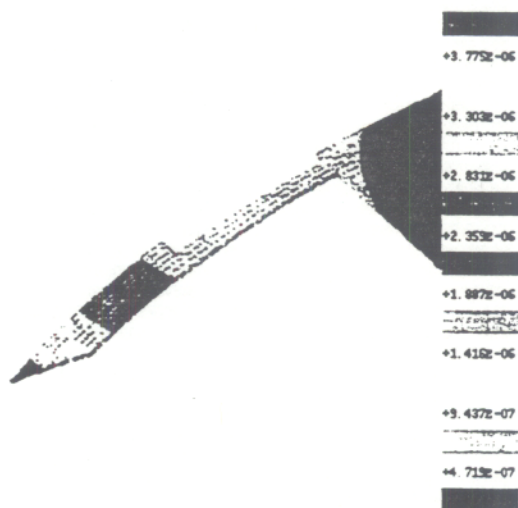


Figure 6. Exaggerated microcantilever deflection for a $100\mu\text{W}$ applied heat load (units in mm).

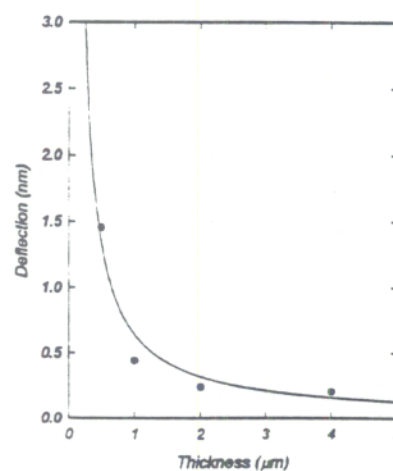


Figure 7. Maximum deflection, z_{max} , as a function of the microcantilever thickness. The points are calculated using a finite element analysis. The solid curve is a fit to Eqn (1).

3. EXPERIMENTAL

A. Microcantilever Ion Milling

A focused ion beam milling system was used in the modification of the commercially available AFM microcantilevers shown in Fig. 1. The system allows real-time viewing of the micro-machining process. Thus the user friendly operator interface was used to simply draw a rectangle around the desired area to be micro-machined. Even though we have had experience ion milling silicon previously, several calibration runs were performed to ascertain the material removal rate for the particular orientation of silicon found in the cantilevers. The most stable conditions produced a material removal rate of $0.027 \mu\text{m}/\text{min.}$, which was used for the entire microcantilever modification process. This corresponds to a gallium ion beam current of $10,550 \text{ pA}$ at 30 KeV . The beam spot size was focused down to 600 nm at the target microcantilever and rastered across the selected area for the required time interval. The nominal starting microcantilever thickness was $4 \mu\text{m}$. Data was taken for this thickness and through subsequent ion milling operations device thicknesses of $2, 1$ which is shown in Fig 8 and 9, and finally $0.5\mu\text{m}$, were produced.

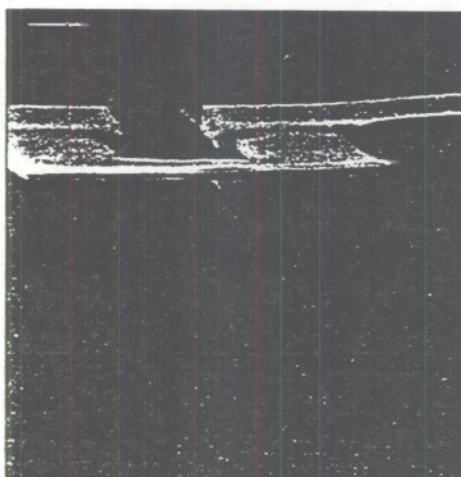


Figure 8. Front view of microcantilever micro-machined to $1 \mu\text{m}$ thickness.

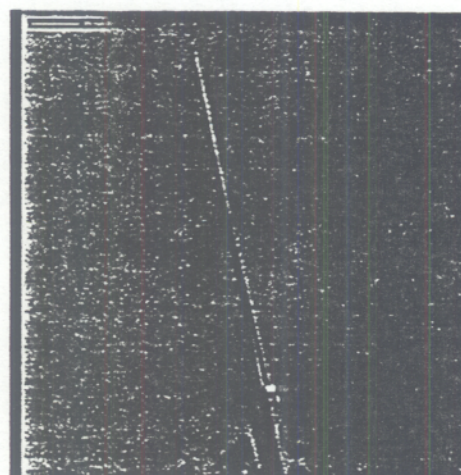


Figure 9. Side view of microcantilever micro-machined to $1 \mu\text{m}$ thickness.

B. IR Radiation Detection Measurements.

We used piezoresistive microcantilevers modified using the procedure described above to perform IR radiation measurements in order to determine the effect of changes in the thickness on the response of the detector. The experimental setup used is depicted in Fig. 10. A heated carbon rod was used as blackbody radiator and served as the IR source. An iris was used to reduce the spatial extent of the blackbody. A mirror was used to collect the emitted IR radiation and focus it on the microcantilever detector. The use of a chopper allowed us to determine the modulation frequency response of the microcantilever. The bending of the microcantilever was determined using an optical detection technique common to AFM.

Bending of microcantilevers can readily be determined by a number of means, including optical, capacitive, electron tunneling, and piezoresistive methods. In this work, we used an optical readout technique for observing microcantilever bending. The approach used was adapted from standard AFM imaging systems. Microcantilevers were mounted in a chip holder (from Digital Instruments) designed for tapping mode AFM, which secured the base of the microcantilever against a small piezoelectric transducer; this chip holder was then mounted on a three-axis translation stage to facilitate fine adjustment of the microcantilever relative to the rest of the experimental apparatus.

All measurements were conducted at ambient temperature and atmospheric conditions.

A diode laser was used in a probe configuration to monitor bending and was focused onto the tip of the microcantilever. A dual-element photodiode displacement detector was used to collect the reflected probe beam. The difference signal from the detector pair as the cantilever tip changed position was used to measure the deflection z_{max} . This signal was directly digitized and stored, or sent to a lock-in amplifier (SR850, Stanford Research Systems) for signal extraction and averaging.

The piezoresistive microcantilever used consisted of a doped layer (boron) in the silicon microcantilever. The design and construction of these microcantilevers is described in detail elsewhere^{16,17}. The piezoresistance of these microcantilever varies when they undergo bending due to thermal stimulation. Assuming a uniform heat dissipation over the entire length, l , of the microcantilever (of thickness t) the change in temperature at the tip, ΔT , ($\approx l^2/2\lambda t dQ/dt$) depends on geometrical factors such as l and t . A temperature change of $\Delta T = 10^{-4}$ K leads to deflections of ~ 1 nm which, in turn, results in a change in electrical resistance of $\Delta R/R \approx 3 \times 10^{-6}$. This can be used to determine the bending of the microcantilever when it absorbs IR radiation.

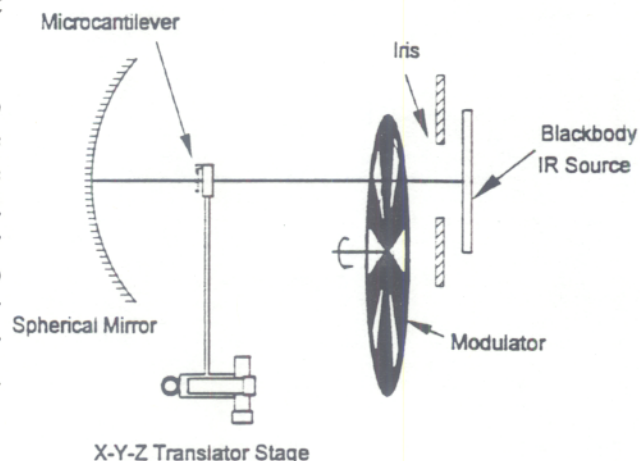


Figure 10. Experimental setup used in the present studies.

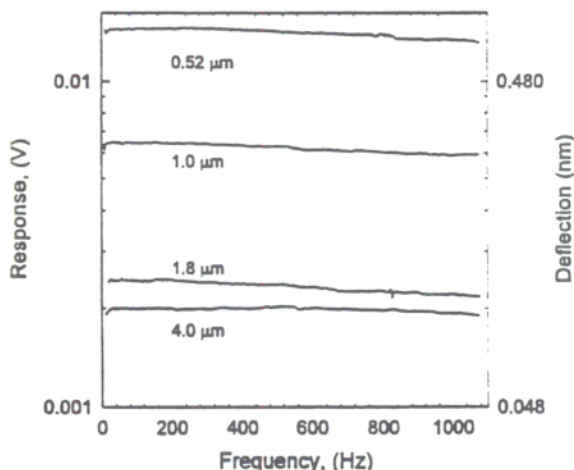


Figure 11. Response (and deflection) of a microcantilever as a function of modulation frequency for different values of thicknesses.

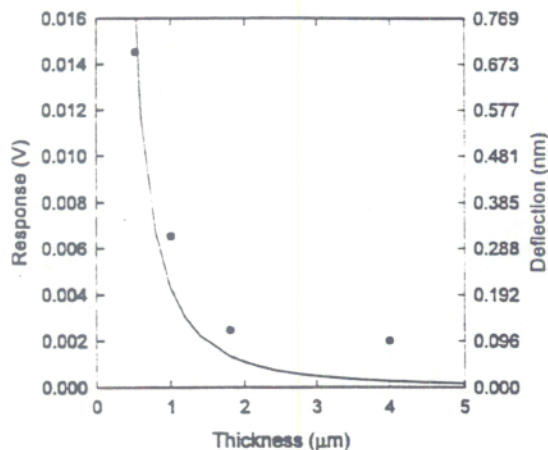


Figure 12. Response (and bending) of the microcantilever detector as a function of thickness. The solid curve is a fit to Eqn (1).

The resonance frequency for different values of t was measured and is plotted in Fig. 3 (closed circles). As it was expected, the resonance frequency decreased with decreasing t . We also measured the response of such microcantilevers exposed to IR radiation from a blackbody radiator. The response was measured as a function of modulation frequencies up to 1200 Hz for four different values of t (Fig. 11).

As can be seen from Fig. 11, the thickness of the microcantilever is very important in the performance of this detector. In Fig 12 we plotted the response (and bending) of the microcantilever detector as a function of thickness. The dependence of the bending on the thickness, t , follows closely a $1/t$ dependence [solid curve in Fig. 12]. For smaller values of t , both the heat conductivity (towards the base of the microcantilever) and heat capacity decrease. Therefore, for the same amount of incident IR power the temperature at the end of the microcantilever becomes higher, resulting in larger deflections (see Fig 12). Since the microcantilevers exhibited no appreciable change in their IR response even for the highest modulation frequencies used, an upper limit for the thermal response times of less than a few ms can be obtained.

4. CONCLUSIONS

As earlier studies⁷ have demonstrated, microcantilevers can be used as uncooled IR detectors with a broadband response. The key element in such detectors is the determination of the bending of the microcantilever induced by the absorption of minute amounts of thermal energy. Clearly the performance of microcantilever based IR detectors can benefit considerably by optimizing their geometry and thermal properties. In the present work we have demonstrated both by modeling and experimental studies that the deflection of a microcantilever can increase substantially (for the same incident power) by using microcantilevers which are thinner and thus possess both smaller thermal mass and better thermal properties. It was also observed that the bimetallic effect is at least as important as the composition of the microcantilever itself. For example, metals with high expansion coefficients such as films of Al, Zn, Pb, or In could be used to increase the thermally induced bending of the microcantilever. Coating the surface of the microcantilever with high emissivity materials (such as gold black) could further improve IR response.

5. ACKNOWLEDGMENTS

The authors would like to thank Kathy Thomas for her valuable assistance in micro-machining in this project. This work was sponsored by the laboratory directors' research and development (LDRD) fund within the Oak Ridge National Laboratory (ORNL). ORNL is managed by Lockheed Martin Energy Research for the U.S. Department of Energy under contract no. DE-AC05-84OR21400. Support was also provided by the Oak Ridge Centers for Manufacturing Technology (ORCMT) through the collaborative use of the user facility of the Ultra-Precision Manufacturing Technology Center. Further support came from the Alexander Hollaender Distinguished Postdoctoral Fellowship Program.

6. REFERENCES

- ¹ R. A. Wood and N. A. Foss, *Laser Focus World*, June, 101 (1993).
- ² A. Rogalski, *Infrared Physics and Technology* **35**, 1 (1994).
- ³ R. A. Wood, *Infrared Technology XXI*, SPIE **2020**, 322 (1993).
- ⁴ C. Hanson, *Infrared Technology XXI*, SPIE **2020**, 330 (1993).
- ⁵ J. L. Miller, *Principles of Infrared Technology* (Van Nostram Reinhold, New York, 1994).
- ⁶ E. L. Dereniak and G. D. Boreman, *Infrared Detectors and Systems* (Wiley and Sons, New York, 1996).
- ⁷ P.I. Oden, P.G. Datskos, T. Thundat, R.J. Warmack, *Applied Physics Letters* (submitted).
- ⁸ D. Sarid, *Scanning Force Microscopy* (Oxford University Press, New York, 1991).
- ⁹ T. Thundat, R. J. Warmack, G. Y. Chen, and D. P. Allison, *Applied Physics Letters* **64**, 2894 (1994).
- ¹⁰ G. Y. Chen, T. Thundat, E. A. Wachter, and R. J. Warmack, *J. Appl. Phys.* **77**, 3618-22 (1995).
- ¹¹ J. R. Barnes, R. J. Stephenson, M. E. Welland, C. Gerber, and J. K. Gimzewski, *Nature* **372**, 79 (1994).
- ¹² J. K. Gimzewski, C. Gerber, E. Meyer, and R. R. Schlittler, *Chemical Physics Letters* **217**, 589 (1994).
- ¹³ J. K. Gimzewski, C. Gerber, E. Meyer, and R. R. Schlittler, in *Micromechanical Heat Sensor: Observation*

- of a Chemical Reaction, Photon and Electrical Heat Pulses*, 1995 (Kluwer Academic Press), p. 123.
- ¹⁴ J. R. Barnes, R. J. Stephenson, C. N. Woodburn, S. J. O'Shea, M. E. Welland, T. Rayment, J. K. Gimzewski, and C. Gerber, *Review of Scientific Instruments* **65**, 3793 (1994).
- ¹⁵ E. A. Wachter, T. Thundat, P. G. Datskos, P. I. Oden, S. L. Sharp, and R. J. Warmack, *Review of Scientific Instruments* (submitted 1996).
- ¹⁶ M. Tortonese, R. C. Barrett, and C. F. Quate, *Applied Physics Letters* **62**, 834 (1993).
- ¹⁷ F. J. Giessibl, *Japanese Journal of Applied Physics* **33**, 3726 (1994).